

## Chapter 6

# Molecular Self-Ordering

This chapter focuses on the self-ordering of organic molecules, since it opens a way to the economic fabrication of nano-structured surfaces in a parallel geometry.<sup>22-24</sup> To use molecular self-ordering it is of fundamental importance to gather knowledge about the monolayer structure and bonding of molecules on metal and semiconductor surfaces. The thin film growth and the formation of ordered monolayers of organic molecules on metal and insulator surfaces have been intensely studied over the last decade.<sup>23-32</sup> It has been found that the self-ordering process sensitively relies on the interplay between molecule-substrate and intermolecular forces. For supramolecular self-assembly, a domination of the non-covalent molecule-molecule interaction over molecule-substrate interactions is assumed, while the substrate provides certain adsorption positions like a checkerboard.<sup>30, 31, 134</sup> However, further detailed knowledge on the correlation between molecular geometry and molecular epitaxial growth is desirable.

To favour the growth of large ordered molecular domains, we chose the symmetry of the investigated systems to meet the requirements for epitaxial growth with single domain orientation on the Cu(111) surface. Thus, the investigated molecules are all showing a six fold symmetry like the substrate. The molecules, already described in the experimental part (section 3.3.2), are: Hexa-*peri*-hexabenzocoronene (HBC, C<sub>42</sub>H<sub>18</sub>), hexa-*tert*-butyl-hexabenzocoronene (HB-HBC, C<sub>66</sub>H<sub>66</sub>), hexaphenylbenzene (HPB, C<sub>42</sub>H<sub>30</sub>), and hexa-*tert*-butyl-hexaphenylbenzene (HB-HPB, C<sub>66</sub>H<sub>78</sub>). The corresponding structure models are

shown in Fig. 3.12. Large polycyclic hydrocarbons like HBC and its derivatives have been proven to be interesting for organic film photovoltaic technology<sup>106</sup> and molecular electronics<sup>107-111</sup>(see section 3.3.2).

In the following the self-ordering and submonolayer growth of the four molecules will be described. Similar preparation conditions for all molecules have been chosen, i.e. 5% to 20% of a saturated monolayer (ML) coverage are evaporated at a flux in the order of  $10^{-4}$  ML/s at a sample temperature of  $(320 \pm 5)$  K. By comparison, the monolayer structures and molecular behaviour upon adsorption can be related to the chemical properties of the molecules. The aim in this chapter is to understand how the variations in the molecular geometry affect lateral ordering, island growth, and molecular adsorption geometry.

## 6.1 Monolayer Structures

### 6.1.1 HPB/Cu(111)

The hexaphenylbenzene molecule (HPB,  $C_{42}H_{30}$ , Fig. 3.12(a)) consists of six phenyl groups, each one connected to the central benzene ring by a  $\sigma$ -bond. Steric hindrance between the outer phenyl groups forbids a planar geometry for the molecule. The phenyl groups of HPB are rotated around the  $\sigma$ -bonds, resulting in a propeller-like shape. An effect of the non-planarity can already be seen in the sublimation temperature of HPB (see Table 3.1), which is about 200 K lower than for the similar but planar HBC (see Fig. 3.12), since only in the latter case strong van der Waals bonding between parallel layers of molecules, similar to the case of graphite, is possible.

When a few percent of a ML of HPB are evaporated on Cu(111) at 320 K sample temperature, large molecular islands with diameters of several 10 nm form. A typical overview showing a part of a HPB island is shown in Fig. 6.1(a). The islands extend often over several terraces and covered terrace steps are straightened due to the presence of the molecules. Such terrace steps and the borders of

molecular islands run preferably along the close-packed directions of the substrate. In general, the adsorption site at step edges is not preferred to molecular agglomerations and molecular islands are found although the step edges are not saturated.

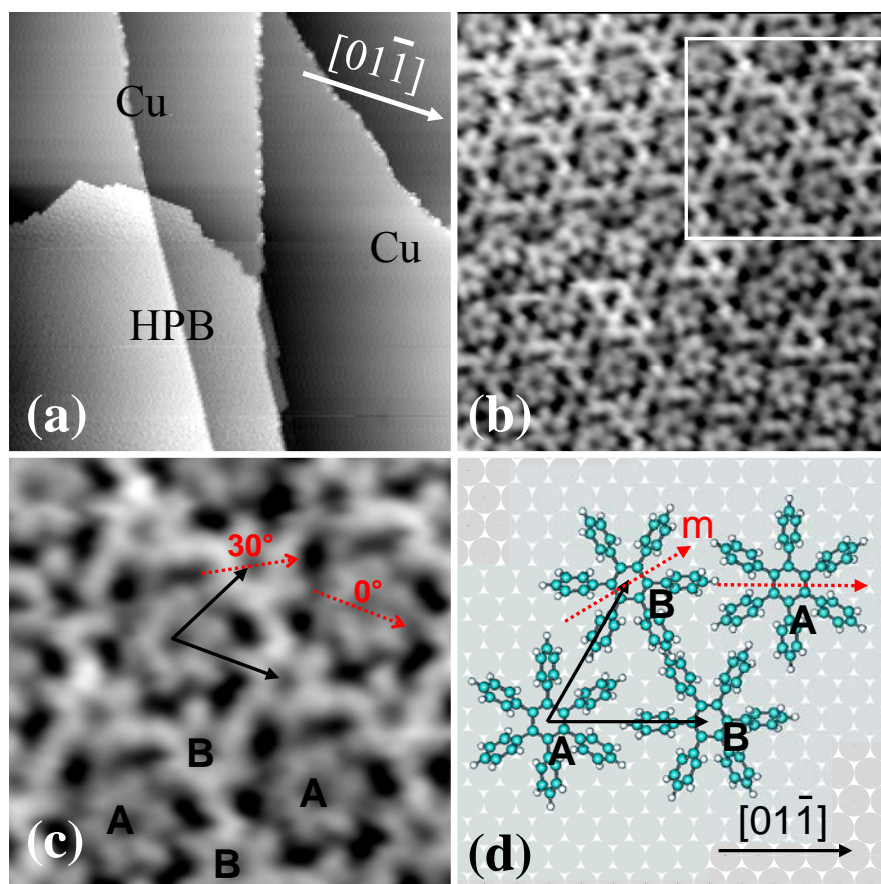


Fig. 6.1. STM measurements of HPB on Cu(111). (a) Typical overview ( $V = -1.0$  V,  $I = 0.2$  nA,  $80 \times 80$  nm<sup>2</sup>), (b) Monolayer structure ( $V = -0.8$  V,  $I = 0.5$  nA,  $10 \times 10$  nm<sup>2</sup>). Molecules appear with different contrast corresponding to the molecular orientation. In the cut out (c) the structure unit cell (solid arrows) is indicated and the molecular orientation, i.e. the angle between  $[01\bar{1}]$  direction and  $\bar{m}$  (dashed arrows), is indicated. Molecules with two different orientations are found, labelled A ( $\bar{m}$  parallel to  $[01\bar{1}]$ ) and B ( $\bar{m}$  rotated  $30^\circ$  with respect to  $[01\bar{1}]$ ). (d) Structure model.

STM images of the monolayer structure with submolecular resolution, (Fig. 6.1(b) and (c)), are sometimes obtained due to a modified tip (in this case molecules or part of them have been picked up to the tip). Single molecules appear as six maxima, corresponding to the six outer phenyl groups around a central minimum at the position of the central planar benzene ring. The distance of two opposite maxima within a molecule is  $(10 \pm 2)$  Å in accordance with the distance of the phenyl rings inside a molecule (8.6 Å). The apparent average height of the molecular layer is 2 Å. The molecules form a hexagonal structure. The unit cell vectors determined by STM are  $|\bar{a}| = |\bar{b}| = (12.8 \pm 0.3)$  Å, the angle between  $\bar{a}$  and  $\bar{b}$  is  $\Phi = (60 \pm 2)^\circ$  and the angle between  $\bar{a}$  and the  $[01\bar{1}]$  direction is  $\Theta = (0 \pm 2)^\circ$ . This corresponds to a  $(5 \times 5)R0^\circ$  structure. However, there exists a larger unit cell consisting of several molecules, since molecules show two different kinds of contrast in STM images. This contrast change presumably has its origin in the orientation of the molecular axis  $\bar{m}$  which may be either rotated  $\sim 0^\circ$  (labelled A) or  $\sim 30^\circ$  (labelled B) with respect to the  $[01\bar{1}]$  direction (see Fig. 6.1(c)). Molecules of type B (which are rotated by about  $30^\circ$ ) usually show a larger apparent height than the molecules of type A ( $0^\circ$  rotation), although the submolecular contrast does strongly depend on tip conditions and tunnelling voltage. The orientation is indicated exemplarily for A and B type molecules in Fig. 6.1(c). In the preferred supramolecular structure, the B type molecules form a honeycomb structure with the A type molecules inside, thus resulting in a  $(\sqrt{3} \times \sqrt{3})R30^\circ$  super unit cell. A structure model based on the experimental results is shown in Fig. 6.1(d).

The STM images show that molecules are adsorbed planar to the (111) surface, i.e. their central benzene ring is oriented surface-parallel. Due to the propeller-like shape, the molecules have two different chiral conformations, corresponding to the rotation of the  $\sigma$ -bonds. However, the chirality of single molecules could not be determined by the STM measurements. It can not be excluded that the found different orientations A and B are connected to different chirality, however, the different orientations alone are sufficient to describe the found structures.

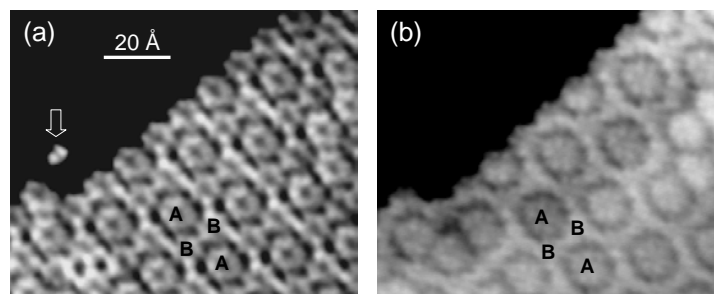


Fig. 6.2. STM images ( $V = 1.0$  V,  $I = 0.2$  nA) of a HPB monolayer with two different STM tips. After image (a) part of an adsorbate (indicated by the arrow) has been picked up by the tip, leading to a drastic change in the contrast, as shown in (b). Molecules of the different orientations are labelled A and B.

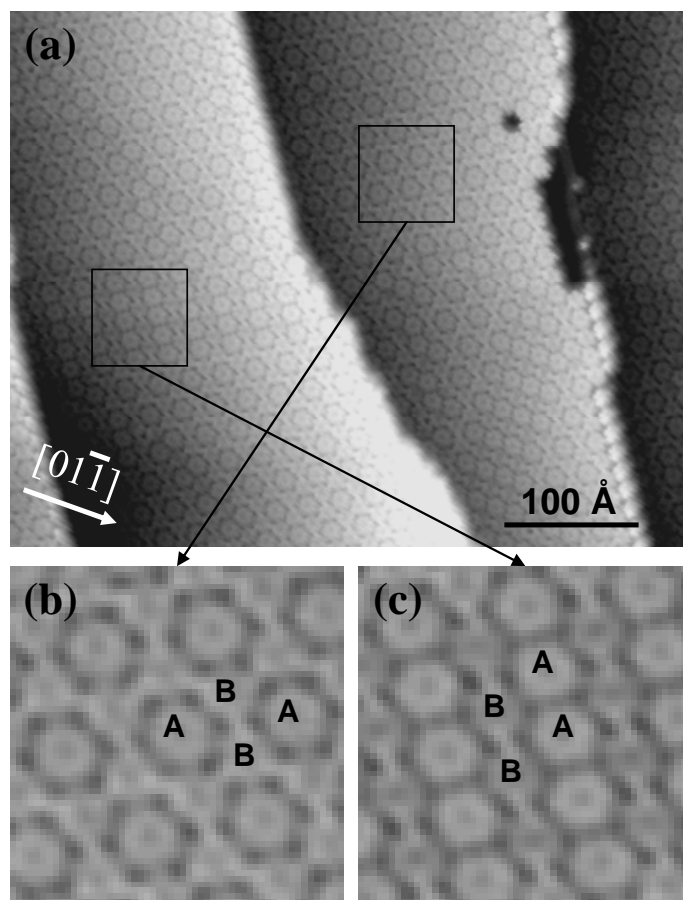


Fig. 6.3. STM measurements of HPB ( $V = 1$  V,  $I = 0.2$  nA). (a) Overview showing several HPB covered terraces (see also background on the cover page).  $(\sqrt{3} \times \sqrt{3})R30^\circ$  superstructure in (b) and  $(2 \times 1)$  superstructure in (c). In (b) and (c) (both  $6 \times 6$  nm<sup>2</sup>) the molecular conformation of different molecules is indicated.

The strong influence of the tip termination on the imaging of HPB molecules is illustrated in Fig. 6.2, where the same surface area is imaged with two differently terminated tips. After imaging Fig. 6.2(a) the tip is positioned above the adsorbate indicated by the arrow and then the tip height is lowered in order to pick up the species and thus change the termination of the tip. The image recorded afterwards, Fig. 6.2(b), shows a different contrast of the molecular structure compared to (a). The contrast between the molecules of type A and B is enhanced, although the tunnelling parameters are not changed with respect to Fig. 6.2 (a).

A tip showing a contrast similar to the one of Fig. 6.2(b) is used to observe the long-range order of the molecular superstructure. The image of a large covered region with high contrast of type A and type B molecules is shown in Fig. 6.3(a). Different molecular superstructures can be observed. The  $(\sqrt{3} \times \sqrt{3})R30^\circ$  structure, shown in Fig. 6.3(b), is dominating. However, long-range order of the superstructure is poor and many defects and antiphase domain boundaries can be observed. Some regions of Fig. 6.3(a) show a different superstructure with a  $(2 \times 1)$  unit cell as shown in Fig. 6.3(c). In section 7.2 I will explain how the molecules within the HPB monolayer can be switched between conformation A and B by means of STM manipulation.

### 6.1.2 HBC/Cu(111)

Hexa-*peri*-hexabenzocoronene (HBC,  $C_{42}H_{18}$ , Fig. 3.12(b)) is a well characterized molecule. Monolayer structures on Cu(111)<sup>32</sup> and Au(111)<sup>32, 117</sup> have been described in detail. HBC is a full planar aromatic system, known to form commensurate monolayer structures on Cu(111) in case of a saturated monolayer coverage<sup>32</sup>.

A typical STM image of a Cu(111) sample covered with a few percent of a monolayer of HBC is shown in Fig. 6.4(a). The step edges are covered with molecules and isolated molecules can be seen on the terraces. Preparations with lower coverage lead to partially covered step edges and uncovered terraces, indicating that the molecules are mobile on the surface at  $T = 320$  K and preferen-

tially adsorb at step edges. Preferred adsorption at step edges, was also observed for benzene<sup>135</sup> and perylene<sup>136</sup> on Cu(111). Nucleation of such molecules at step edges presumably arises from the interaction of adsorption-induced molecular dipoles<sup>135</sup> with the intrinsic dipoles of metal step edges, which are due to the Smoluchowski effect<sup>137</sup>.

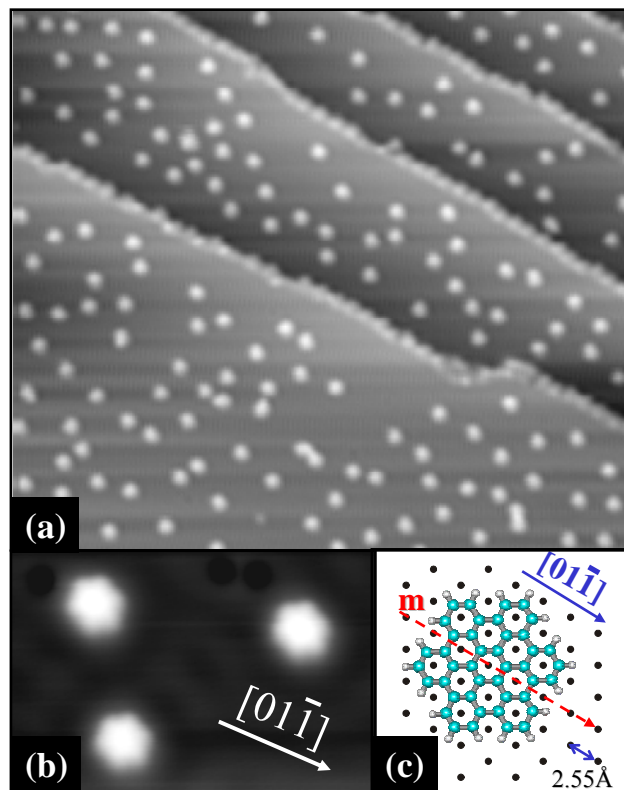


Fig. 6.4. (a) STM image of HBC on Cu(111), ( $V = 0.8\text{ V}$ ,  $I = 0.2\text{ nA}$ ,  $60 \times 60\text{ nm}^2$ ), the step edges are saturated, molecules are found isolated on the terraces. (b) Single molecules ( $V = -0.1\text{ V}$ ,  $I = 0.2\text{ nA}$ ,  $9 \times 5\text{ nm}^2$ ). (c) Corresponding adsorption model. The molecular axis  $\vec{m}$  is indicated.

Adsorption on the terraces takes place only if the coverage is high enough to saturate all step edges, as in Fig. 6.4(a). In this case, the molecules on the terraces are always found separated. Even annealing of the sample at 470 K after evaporation, in order to increase the molecular mobility, does not lead to any molecular agglomeration. The molecules do not form molecular islands in submonolayer coverage although they are mobile on the surface, indicating a lacking of attrac-

tive intermolecular forces. The same effect has been reported also for other planar polycyclic hydrocarbons, like for example perylene<sup>26, 30</sup>, coronene<sup>26, 138</sup>, pentalene<sup>136</sup> and the almost planar decacyclene<sup>28</sup> on various noble metal surfaces.

Single HBC molecules on a Cu(111) terrace appear in STM images (Fig. 6.4(b)) as hexagons with an apparent height of 1.7 Å (tunnelling bias between -0.5 V and 0.5 V). The lateral dimensions measured from half maximum to half maximum are 14 Å from corner to opposite corner and 13 Å from side to opposite side, respectively, in good correspondence to the van der Waals dimensions of the molecule (Fig. 3.12(b)). The orientation of the hexagons is identical for all molecules and reflects the molecular orientation on the surface. The molecules are oriented with the molecular axis  $\bar{m}$  parallel to the close-packed directions of the Cu surface, thus allowing equal positions of all carbon rings inside the HBC molecule with respect to the surface unit cell. A model of adsorption is shown in Fig. 6.4(c). The molecular orientation of the single molecules is the same as found in the case of a saturated monolayer<sup>32</sup>.

### 6.1.3 HB-HBC/Cu(111)

The larger hexa-*tert*-butyl-hexabenzocoronene molecule, (HB-HBC, C<sub>66</sub>H<sub>66</sub>, Fig. 3.12(c)) is formed by substitution of the six free para position of the HBC core by six *tert*-butyl (C<sub>4</sub>H<sub>9</sub>) groups. The influence of such spacer groups has been already studied in the group of Besenbacher in case of the decacyclene (DC) molecule, which has been investigated with and without spacer legs on Cu(110).<sup>27, 28</sup> The spacer groups are known to elevate the molecular core with respect to the planar metal surface, decreasing the surface interaction of the molecular core and therefore lowering the diffusion barrier. On the other hand, adsorption geometry with a large overlap between molecular  $\pi$ -orbitals and metal surface is preferred. The overlap can be increased, despite the spacer legs, by adsorption at step edges or by formation of nanostructures under the molecular core, as recently reported for HB-DC on Cu(110)<sup>27</sup> and for Lander molecules on Cu(110)<sup>95</sup> and as described in section 4.2 for Cu(211).



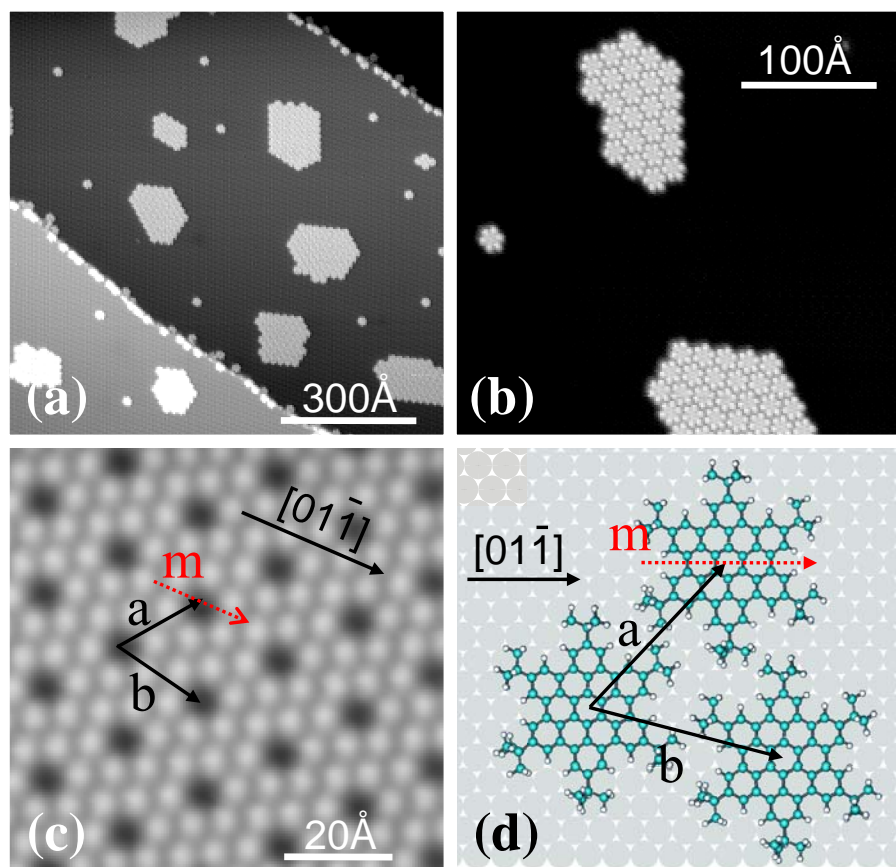


Fig. 6.5. STM measurements of HB-HBC on Cu(111). (a) Typical overview after preparation at 320 K. Several small islands and isolated molecules can be seen. (b) Two islands of different orientation and one separated molecule. (c) A molecular monolayer with indicated unit cell vectors and molecular axis  $\vec{m}$ . (d) Structure model.

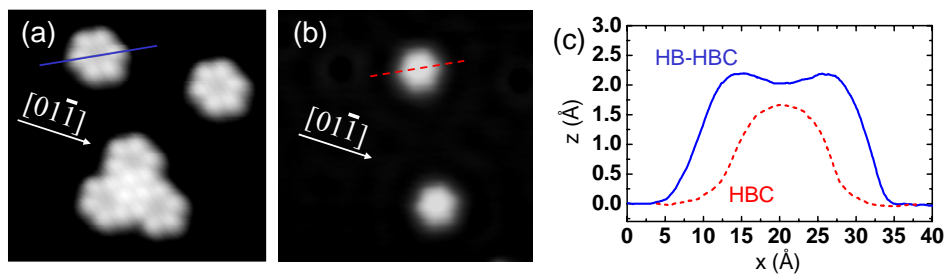


Fig. 6.6. (a) Two single HB-HBC molecules and a cluster of three molecules. (b) Single HBC molecules for comparison. Both STM images at  $V = 100$  mV,  $I = 0.1$  nA, size:  $10 \times 10$  nm<sup>2</sup>. The indicated lines display the position of the line profiles shown in (c).

Fig. 6.5(a) shows a Cu(111) sample with a coverage of approximately 0.1 ML of HB-HBC. The step edges are saturated and molecules on the terraces are found separated or in small islands with a typical size of 10-100 molecules.

The Cu terraces are equally covered with molecular islands. In Fig. 6.5(b) and (c) such islands are shown with submolecular resolution. Each molecule displays six maxima corresponding to the six *tert*-butyl spacer groups of the molecule. In Fig. 6.5(c) the molecular unit cell vectors and the orientation  $\bar{m}$  of the molecular axis are indicated. The molecular axis  $\bar{m}$  is parallel to the  $[01\bar{1}]$  direction of the substrate. The unit cell vectors of the molecular layer determined with STM are  $|\bar{a}| = |\bar{b}| = (18.4 \pm 0.3) \text{ \AA}$ . The angle between  $\bar{a}$  and  $\bar{b}$  is  $\Phi = (60 \pm 2)^\circ$  and the angle between  $\bar{a}$  and the  $[01\bar{1}]$  direction is  $\Theta = \pm (14 \pm 3)^\circ$ . Since no superstructure or modulation is observed and a commensurate structure is possible within the experimental errors I propose a  $\begin{pmatrix} 6 & -2 \\ 2 & 8 \end{pmatrix}$  structure, corresponding to a nearest neighbour distance of  $|\bar{a}| = |\bar{b}| = 18.4 \text{ \AA}$ ,  $\Phi = 60^\circ$ , and  $\Theta = 13.9^\circ$ .

In conclusion HB-HBC molecules form islands with a  $(\sqrt{52} \times \sqrt{52})R14^\circ$  structure on Cu(111). The proposed structure model is shown in Fig. 6.5(c). It follows that islands with two different orientations ( $\pm 13.9^\circ$ ) are possible, i.e.  $\begin{pmatrix} 6 & -2 \\ 2 & 8 \end{pmatrix}$  and  $\begin{pmatrix} 8 & 2 \\ -2 & 6 \end{pmatrix}$ . In Fig. 6.5(b) islands of both kind can be seen. In one case the unit cell is rotated by  $+14^\circ$  and in the other case by  $-14^\circ$  with respect to the  $[01\bar{1}]$  direction. The different molecular islands can also be recognized in images without molecular resolution (Fig. 6.5(a)) by observing the preferred direction of their edges, which run in an angle of  $+14^\circ$  or  $-14^\circ$  with respect to the close-packed directions of the substrate.

Isolated molecules are shown in Fig. 6.6(a) and a line scan across a molecule is shown in Fig. 6.6(c). The apparent height of the maxima, corresponding to the butyl side groups is  $2.2 \text{ \AA}$ . The distance of two opposing maxima within one molecule is  $13 \text{ \AA}$ , corresponding to the distance of the *tert*-butyl groups inside the

molecule. The board of the molecule has an apparent height of 2.0 Å, which is larger than the 1.7 Å of the HBC core molecule alone.

All HB-HBC molecules are oriented in the same direction with respect to the Cu(111) substrate, with the molecular axis  $\bar{m}$  parallel to the  $[01\bar{1}]$  direction. This is observed for both isolated molecules and for those forming islands. Since the orientation of the molecular board is the same as found for the adsorption of HBC, the two molecules presumably adsorb at identical sites of the substrate.

#### 6.1.4 HB-HPB/Cu(111)

The hexa-*tert*-butyl-hexaphenylbenzene molecule, (HB-HPB,  $C_{66}H_{78}$ , Fig. 3.12(d)) corresponds to a HPB molecule with six additional *tert*-butyl spacer groups.

In submonolayer coverage HB-HPB forms large ordered islands, covering few terraces completely and leaving most Cu terraces and step edges uncovered. An overview of this situation is shown in Fig. 6.7(a). The long range order of these molecular structures is very good and defect free islands of about 1000 Å in diameter are observed. Fig. 6.7(b) and (c) show the HB-HPB structure with molecular and submolecular resolution, respectively. Like in the case of HPB, the island border lines preferably run along the close-packed directions of the substrate. In contrast to HPB, HB-HPB islands do rarely extend over steps or cover steps. HB-HPB islands are terminated by step edges and usually the islands do not extend to the edge of the step, but a space narrower than one molecular width remains uncovered in front of the step edge. This is observed for both up and down step edges, as can be seen in Fig. 6.7(b). Each depression in Fig. 6.7(b) corresponds to the HPB core of a molecule. The depression is surrounded by six maxima, which are resolved in Fig. 6.7(c) and correspond to the positions of the *tert*-butyl side groups. Contrary to HB-HBC (Fig. 6.5(c)), the molecular board shows characteristic contrast inside. The central benzene ring of the HPB core is imaged as a distinct minimum (Fig. 6.7(c)).

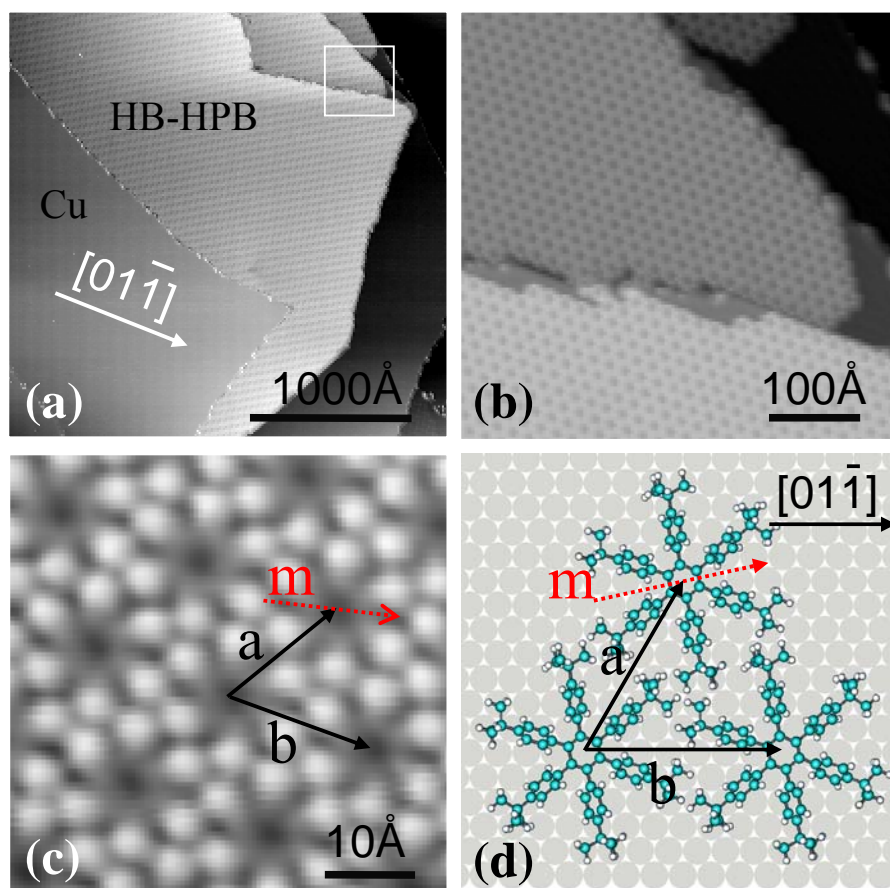


Fig. 6.7. STM measurements of HB-HPB on Cu(111) for decreasing image sizes ( $V = 0.8$  V,  $I = 0.2$  nA). (a) Overview. Molecule covered terraces are identified by Moiré patterns. Defect-free monolayers are resolved with molecular resolution in (b) and with submolecular resolution in (c). The six *tert*-butyl groups appear as maxima while the central phenyl ring is observed as a depression. The structure unit cell vectors and the molecular axis  $\bar{m}$  are indicated. (d) Structure model.

The monolayer structure of HB-HPB differs from the structure of HB-HBC, although both molecules are almost identical in size and are equipped with the same side groups. The unit cell vectors of the HB-HPB structure are aligned with the substrate and are measured as  $|\bar{a}| = |\bar{b}| = (18.0 \pm 0.3)$  Å corresponding to  $(7 \times 7)R0^\circ$  growth on Cu(111). However, the symmetry axis of single molecules inside the monolayer is not aligned with the substrate symmetry planes. The molecules are oriented uniformly within one island, with the molecular axis

rotated  $(11 \pm 3)^\circ$  with respect to the  $[01\bar{1}]$  direction of the substrate. Therefore two domains with identical unit cell vectors but different chirality can be observed: One domain in which all molecules are rotated  $11^\circ$  clockwise and one domain in which all molecules are rotated  $11^\circ$  anticlockwise with respect to the  $[01\bar{1}]$  direction. A structure model is shown in Fig. 6.7(d). Islands with different chirality, i.e. molecular orientation, can be observed in Fig. 6.8.

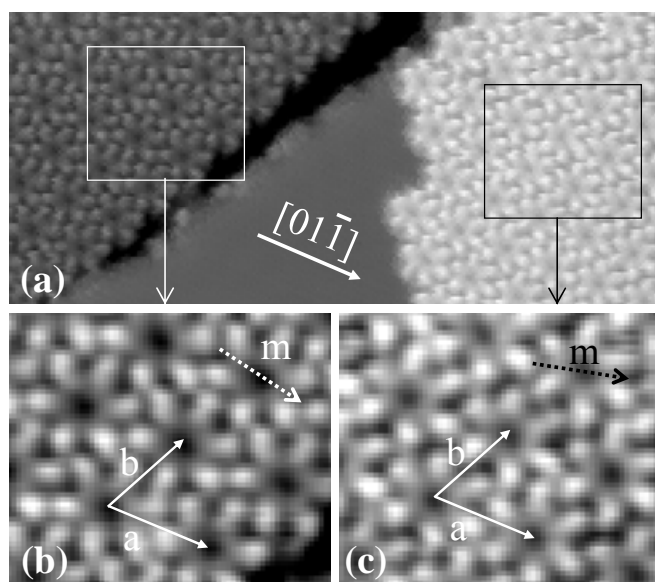


Fig. 6.8. Two domains of HB-HPB with different chirality. In (a) both domains are shown in one STM image ( $V = -0.1$  V,  $I = 0.2$  nA,  $23 \times 11$  nm<sup>2</sup>). Regions in both domains are shown enlarged in (b) and (c), the unit cells are indicated. Note that the unit vectors of both cells are identical; the domains differ only in the orientation of the molecular axis  $\bar{m}$  (dashed arrows).

Due to the propeller shape of the HPB core, the HPB and HB-HPB molecules itself show a chirality when adsorbed on the metal surface. However, it was not possible to distinguish the expected enantiomers. The chirality of the single molecules is probably not connected with the observed chirality of HB-HPB domains, which has its origin in the (clockwise or anticlockwise) rotation of the molecular axis with respect to the  $[01\bar{1}]$  orientation.

## 6.2 Comparison of Molecular Growth

All the investigated molecules form commensurate monolayer structures on Cu(111). A comparison between the submonolayer growth of all four molecules is shown in Table 6.1. The entirely planar HBC molecule, missing intermolecular van der Waals forces strong enough to form islands in the submonolayer regime, is forced in its hexagonal close-packed structure only for the completely saturated monolayer. The missing of out-of-plane molecular bonds is probably the reason for the small attractive intermolecular interaction, observed for several fully planar hydrocarbons on noble metal surfaces<sup>26, 138</sup>.

Molecule	Monolayer structure	NN distance	Orient. of $m$ ( $\Phi$ )	Number of domains	Submonolayer growth	Preferred adsorption sites
HBC	$(\sqrt{31} \times \sqrt{31})R \pm 9^\circ$	14.2 Å	$0^\circ$	2 orient.	separated molecules	step edges
HB-HBC	$(\sqrt{52} \times \sqrt{52})R \pm 14^\circ$	18.4 Å	$0^\circ$	2 orient.	small islands	step edges
HPB	$(5 \times 5)R0^\circ$	12.6 Å	$0^\circ/30^\circ$	several super-structures	large islands	molecular islands and step edges
HB-HPB	$(7 \times 7)R0^\circ$	17.9 Å	$\pm 11^\circ$	2 chiral	large islands	molecular islands

Table 6.1. Comparison of monolayer structures of all four investigated molecules on Cu(111), evaporated at 320 K sample temperature. The structure of HBC is only formed in the case of a saturated monolayer<sup>32</sup>.

The molecules HBC and HB-HBC are always oriented with their molecular axis parallel to the close-packed directions of the Cu(111) substrate. This can be understood due to the interaction of the planar molecular board, which fits the substrate very accurately in its lattice constant, allowing equal adsorption sites for all aromatic rings of the molecular board.

The molecules with HPB core (HPB and HB-HPB), having only one aromatic ring planar to the surface, seem to face only little constraint on molecular orientation due to molecule-substrate-interactions. HB-HPB forms large molecu-

lar domains with uniform molecular orientation. The molecules are tilted by  $\pm 11^\circ$  with respect to the  $[01\bar{1}]$  direction, allowing a very dense packing of molecules, which are interlocked. The molecules form a  $(7 \times 7)$  structure, i.e. the unit cell vectors are aligned with the substrate and the packing is denser compared to the HB-HBC structure. For HB-HPB, two domains of different chirality are observed (Fig. 6.8), while there are two domains with different orientation in the case of HBC<sup>32</sup> and HB-HBC (Fig. 6.5(b)). Due to the determination of the molecular orientation by the strong interaction between HBC board and metal surface, the HBC and HB-HBC monolayer structures are not packed as dense as in the case of the HPB core, which allows molecular interlocking and rotation on the Cu(111) surface.

In the case of the HPB molecule, the molecular axis is rotated either  $0^\circ$  or  $30^\circ$  with respect to the  $[01\bar{1}]$  direction, leading to  $(\sqrt{3} \times \sqrt{3})R30^\circ$ ,  $(1 \times 2)$  or disordered domains, where the first seems to be the preferred superstructure.

The molecular orientation of HPB and HB-HPB originates from the intermolecular interactions. In HB-HPB, the intermolecular interactions are highly likely CH- $\pi$  hydrogen bonds between one CH of a *tert*-butyl group and the closest phenyl ring of the neighbour molecule. The commensurate molecular structure and the adjustment of the molecular orientation by intermolecular forces can be explained by a fixed adsorption position of the molecule on the one hand and little constraint of the substrate on the molecular orientation on the other hand. In that aspect the situation is similar to the one of PTCDA on Ag(111), one of the best known examples of commensurate organic epitaxy.<sup>25</sup> It has been pointed out by Eremtchenko et al. that the existence of a single pinning centre is one of the reasons leading to the extremely well ordered growth observed for PTCDA.<sup>30</sup> In the case of HB-HPB, such a centre is presumably the central benzene ring, which is the only aromatic part of the molecule that is parallel to the surface thus allowing a large overlap of the  $\pi$ -system with the metal. Like PTCDA on Ag(111) also HB-HPB on Cu(111) shows almost perfectly ordered commensurate growth.

In case of HBC and HB-HBC, the molecules are always oriented with respect to the substrate, pointing on the existence of several binding centres. The pinning

sites of hydrocarbons are most likely located at those aromatic  $\pi$ -systems, which are parallel to the surface. This is supported by the finding that the surface parallel  $\pi$ -systems are also the main responsible for surface state scattering as shown in the case of Lander molecules Cu(111) (see section 5.3).

The different weighting of molecule-metal with respect to intermolecular forces becomes noticeable in the preferred adsorption sites. In the case of HBC the domination of adsorbate-substrate interaction leads to no island formation and molecules preferably adsorb at high coordinated sites of the substrate, like step edges and kink sites. In the case of HB-HBC the *tert*-butyl side groups induce attractive intermolecular van der Waals forces. The preferred adsorption site however is still at step edges, but small molecular islands are formed if all step edges are saturated.

Due to the non-planarity of the HPB board, the molecule-metal interaction is weakened in the cases of HPB and HB-HPB. For both molecules the adsorption site is determined by the substrate, causing commensurate growth, but the molecular orientation is mainly determined by the intermolecular interactions. In this aspect, the influence of the intermolecular interaction is becoming stronger, as can also be seen in the fact that adsorption at substrate step edges is not preferred over adsorption at molecular islands.

The stronger bonding to the substrate in case of the HBC core compared to HPB could also be measured by means of STM induced lateral manipulation. The minimum resistance needed to manipulate single isolated molecules under equal conditions is about 5 orders of magnitude smaller in the case of HBC and HB-HBC compared to HPB and HB-HPB, respectively (see section 7.1). Thus the tip has to be about 5 Å closer to the surface for the lateral manipulation of a molecule with HBC core compared to a molecule with HPB core. This is a clear indication of a higher diffusion barrier and a stronger molecule-metal bonding in the case of the HBC core. The fact that manipulation parameters are approximately equal for HBC compared to HB-HBC on the one hand and HPB compared to HB-HPB on the other hand, indicates little influence of the *tert*-butyl legs on the molecule-substrate bonding. The para *tert*-butyl side groups main axis are in the molecules



main plane and are not large enough to elevate the molecular board significantly from its equilibrium position with respect to the surface (contrary to the meta di-*tert*-butyl-phenyl groups of Lander molecules<sup>96,98</sup>).

A clear correspondence between the degree of order and the balancing between molecule-metal and intermolecular interactions can be made out for the investigated molecules: The more the adsorption is governed by intermolecular interaction, the better is the structural order and the larger the size of defect free domains. However, adsorbate-substrate interactions remain important for commensurate growth and the best molecular order is achieved for molecules with a single pinning centre.

### 6.3 Conclusions

An LT-STM study of the submonolayer growth of four derivatives of hexa-*peri*-hexabenzocoronene on Cu(111) has been presented in this chapter and structure models of the observed ordered monolayer structures have been proposed.

The most important results are summarized in Table 6.1. When going down in Table 6.1, the weighting of the forces on the molecules gradually shifts from a strong domination of molecule-substrate forces towards the domination of intermolecular interactions. This shift comes along with an improved molecular ordering. The largest defect free domains have been found for HB-HPB, a molecule with presumably one pinning centre, allowing the orientation of the molecules to be adjusted by intermolecular forces. In this special case chiral domains are formed, which are only distinguished by their chirality (induced by the molecular orientation), apart from that showing the identical structure matrix and uniform structure orientation.

Thanks to the systematic choice of molecules it is possible to assign the properties regarding self-ordering to specific chemical groups inside the molecule. It is found that *tert*-butyl groups induce intermolecular attraction, while their influence on the molecule-substrate bonding is negligible. The planar aromatic HBC on the

other hand strongly bonds to the substrate inducing a fixed orientation, while the HPB core bonds only at the central position, allowing a rotation of the molecule in the absence of other pinning centres. It can be concluded that the strongest molecular-substrate interactions of these molecules are mediated by the delocalized  $\pi$ -systems of aromatic molecular groups, which are oriented parallel to the surface. This finding is also supported by the predominant scattering of such molecular parts as demonstrated for Lander molecules (see section 5.3). On the other hand, intermolecular forces are mediated by aromatic parts, which are not oriented parallel to the surface, and by the hydrogen saturated *tert*-butyl groups. The investigation leads to an identification of the chemical groups responsible for anchoring to the substrate, for molecular orientation, and intermolecular bonding. Such information is useful for the general expectation of adsorption in the case of similar organic-metal systems and thus will help to improve the design of molecules with regard to their self-ordered monolayer arrangement. In this aspect, the investigation of a larger diversity of molecular subgroups will be of general interest. In particular, the effect, in terms of molecular ordering, of the substitution of carbon atoms by nitrogen atoms, precisely the substitution of one phenyl side group ( $C_6H_5$ ) by a pyrimidine group ( $C_3N_2H_3$ ), is currently under investigation.